

THE ROLE OF SIGM AND GLPF ON CELL WALL ACTIVE ANTIBIOTIC  
SUSCEPTIBILITY IN *BACILLUS ANTHRACIS* STERNE

By

Graham Garrett Ellis

Submitted in partial fulfillment of the  
requirements for Departmental Honors in  
the Department of Biology  
Texas Christian University  
Fort Worth, TX

May 4, 2020

THE ROLE OF SIGM AND GLPF ON CELL WALL ACTIVE ANTIBIOTIC  
SUSCEPTIBILITY IN *BACILLUS ANTHRACIS* STERNE

Project approved by:

Supervising Professor: Shauna McGillivray, Ph.D.

Department of Biology

Giridhar Akkaraju, Ph.D.

Department of Biology

Heidi Conrad, Ph.D.

Department of Chemistry and Biochemistry

## ABSTRACT

The bacterium *Bacillus anthracis*, the causative agent for the disease anthrax, possesses two plasmids that contribute significantly to virulence. Besides plasmids, certain chromosomal genes also contribute. In previous studies, our lab discovered that the chromosomally encoded *clpX* gene is essential for virulence in *B. anthracis*. ClpX is an ATPase that is part of the ClpXP proteasome found in many bacteria. Loss of ClpX in *B. anthracis* Sterne results in increased susceptibility to cell wall targeting antibiotics like penicillin and daptomycin. However, the mechanism behind ClpX's role in antibiotic resistance is not well understood and it is likely that multiple pathways are affected by the loss of this global protease. We recently conducted a microarray to find which genes are up or down regulated in  $\Delta$ ClpX compared to wild-type (WT) *B. anthracis*. 119 genes had disrupted regulation and several of these had been connected to cell-wall active antibiotics like penicillin. In this study, we focused on three of these genes: *msrA*, *glpF*, and *sigM*. We confirmed the microarray results and showed that *msrA*, *glpF*, and *sigM* gene expression in our  $\Delta$ ClpX strains significantly differs from the wild-type *B. anthracis* Sterne via QPCR. Insertional knockout mutants were made for *glpF* and *sigM* to test whether these genes were necessary for antibiotic resistance. We found removing *sigM* results in increased susceptibility to penicillin, but no conclusive results could be drawn for daptomycin. We tested the virulence of both mutants in our invertebrate animal model *G. mellonella* and found notable decreases in virulence for both  $\Delta$ SigM and  $\Delta$ GlpF. Thus, SigM appears to also mediate antibiotic resistance and may at least partially account for the loss of resistance seen in the  $\Delta$ ClpX mutant. Further studies will be needed to confirm the exact role in mediating antimicrobial resistance and potentially virulence for *B. anthracis*.

### ACKNOWLEDGEMENTS

I would like to acknowledge the Texas Christian University College of Science and Engineering for helping to fund this research through the SERC grant. I would also like to thank my fellow lab mates and our lab's graduate student, Lang Zou. Finally, I would like to recognize and thank Dr. Shauna McGillivray for her training, support, and commitment without whom this thesis would not be possible.

TABLE OF CONTENTS

INTRODUCTION .....	1
METHODS .....	6
QUALITATIVE REVERSE TRANSCRIPTASE PCR (QPCR) .....	6
PRIMER EFFICIENCY .....	7
INSERTIONAL MUTANTS .....	7
MINIMUM INHIBITORY CONCENTRATION ASSAY .....	10
GALLERIA MELLONELLA VIRULENCE ASSAY .....	11
RESULTS .....	12
DISCUSSION .....	20
REFERENCES .....	24

## INTRODUCTION

*Bacillus anthracis* is a gram-positive rod-shaped bacterium and the etiological agent of the disease anthrax. Anthrax is a zoonotic disease transmitted to humans through contact with infected animals, like sheep, or animal products [1, 2]. Anthrax infections can result in death depending on the method of entry and whether the infection becomes systemic [1]. Cutaneous infections, which account for 95 percent of anthrax infections in the US, involve the introduction of endospores through cuts or abrasions. Most exposures occur on the head, neck and extremities. After the appearance of a papule, the lesion forms a necrotic vesicle that leaves a black eschar. Lesions resolve in 80 to 90 percent of cases without complications. However, there are still risks. The most common route of infection for anthrax meningitis, a rare complication, is through the skin. Gastrointestinal anthrax involves ingestion of endospores with symptoms occurring two to five days post-ingestion. Gastrointestinal infection always leads to ulceration as well as symptoms like fever and abdominal pain. Gastrointestinal anthrax can be fatal. Inhalational anthrax occurs after inhaling endospores. Incubation times can extend up to six weeks after exposure. Symptoms include fever, cough, dyspnea, and chills. Even with treatment, inhalational anthrax can be fatal [1].

To prevent infection and death via *B. anthracis*, several different preventative measures and treatments are available. An FDA-approved vaccine is available for individuals at risk of exposure to endospores. This vaccine uses aluminum hydroxide preparation of the protective antigen of the *B. anthracis* Sterne strain. *B. anthracis* Sterne is an attenuated strain that can synthesize exotoxins but not the capsule. The current vaccine requires administration at two and four weeks followed by doses at six, twelve, and eighteen months. Afterwards, boosters are

required every year. Researchers continue to develop new vaccines, which are currently being tested, for better protection and an easier administration schedule [1]. If individuals are suspected of exposure, a six-week course of doxycycline, penicillin or ciprofloxacin can be utilized. Even with these treatments, certain anthrax infections such as meningeal, gastrointestinal or inhalational anthrax are still highly dangerous [1]. To compound the issue of treatment, antibiotic resistance can be generated experimentally to several different kinds of antibiotics including fluoroquinolones like ciprofloxacin as well as, in one study, doxycycline [3]. Furthermore, cases of penicillin and doxycycline resistance have been reported, although they appear to be from engineered strains [3].

Along with forming resistance to antibiotics, *B. anthracis* can also withstand many dangerous environmental factors. This is accomplished through the endospore that the bacteria can form. As an endospore, *B. anthracis* cannot divide, but it can survive against drying, heat, ultraviolet light, and large numbers of disinfectants. This hardiness allows spores to survive dormant in soil for many decades. Disinfection of contaminated areas can be achieved using formaldehyde [1]. For example, on Gruinard Island, the spores of *B. anthracis* left over after biological weapon tests in 1942 and 1943 were inactivated using 5 percent formaldehyde in seawater. Without decontamination, measuring indicated that spores would have remained “well into the 21<sup>st</sup> century” [2].

While the endospore of *B. anthracis* protects it from environmental factors like heat, the capsule protects it from an infected host’s immune system. The capsule is coded on three genes, *capB*, *capC*, and *capA*, which reside on one of the two plasmids in *B. anthracis*: pXO2. Together the products form a protective capsule which prevents the phagocytosis of the bacteria [1]. While the plasmid pXO2 prevents the destruction of the bacteria, the plasmid pXO1 produces

exotoxins. pXO1 contains genes for lethal factor, edema factor and protective antigen. Both lethal factor and edema factor bind to protective antigen to form exotoxins. These toxins interfere with the host immune response. Edema toxin interferes with neutrophil function. Lethal toxin causes macrophages to secrete Tumor Necrosis Factor  $\alpha$  and Interleukin-1 $\beta$ , both of which contribute to host death in systemic anthrax. Together, pXO1 and pXO2 are major virulence factors for *B. anthracis* [1].

While the pXO1 and pXO2 plasmids contribute significantly to virulence, specific genes in the chromosome of *B. anthracis* have also been found to affect virulence. Specifically, the ClpX protein, which serves as a part of the ClpXP proteolytic complex [4]. ClpXP plays a role in protein folding, activation, or disaggregation. ClpXP consists of a central ClpP core and one or two ClpX ATPases [5]. ClpX helps unfold the tertiary structures of recognized proteins and moves the unfolded protein into the proteolytic ClpP, where the protein is further degraded into smaller peptide fragments [6]. ClpX also serves as a chaperone, helping newly formed proteins assume the correct shape without misfolding or aggregating [6, 7]. The Clp ATPases allow ClpP to have proteolytic activity. ClpXP has tremendous reach in affecting genes throughout many different species of bacteria. The ClpXP protease helps dispose of denatured proteins that accumulate at high temperatures seen in heat shock and other similarly stressful events but it can also regulate transcriptional regulators and various enzymes [5]. In *S. mutans*, deletion of ClpP and ClpX resulted in changes to 10 percent of the genome for each deletion [8]. In *E. coli*, ClpXP helps control stress adaptation, cell division, and DNA damage repair (like with the DNA repair protein RecN) [6, 7]. Furthermore, disrupting Clp proteins can result in improper filamentation as well as irregular cell walls [5].



In *B. anthracis* Sterne, previous work in our lab found that the loss of the *clpX* gene increased susceptibility to cell-wall active antibiotics such as penicillin and daptomycin [9, 10]. Penicillin affects the actions of PBPs (penicillin binding proteins) that form the cell wall through transpeptidation and carboxypeptidation [11]. Daptomycin, when associated with calcium, causes depolarization and permeabilization of the bacterial cell membrane resulting in cell death. While the known method of bactericidal activity of daptomycin does not necessarily directly affect the cell wall, several known daptomycin resistance mechanisms are due to modification of the cell wall specifically by changing surface charge [12]. Other antibiotics like erythromycin and ciprofloxacin which do not target the cell wall did not result in increased bacterial cell death over their wild-type (WT) counterparts [9]. The increased susceptibility to cell-wall active antibiotics indicates a relationship between *clpX* and the cell wall.

While the effect of *clpX* on *B. anthracis*' antibiotic susceptibility is documented [8,9], the mechanism behind it is not. It is unlikely that the ClpXP protease is directly modulating antibiotic resistance or cell wall morphology but rather is influencing expression of other proteins that are more directly playing a role. Given the Clp protease complex's large global effect on bacteria, analyzing the changes in expression of genes in WT *B. anthracis* compared to a mutant strain with the ClpX gene removed could identify the genes affected by *clpX* that regulate antibiotic susceptibility. As such, the global gene expression of WT *B. anthracis* and the *clpX* deleted strain  $\Delta$ ClpX *B. anthracis* were examined using a microarray, which compared relative levels of each gene between WT and  $\Delta$ ClpX. One hundred and nineteen genes were significantly up or down regulated in  $\Delta$ ClpX compared to WT *B. anthracis* [10]. Several of those genes were related to the cell wall. Two of those genes related to the cell wall, *lrgA* and *lrgB*, are part of an operon *lrgAB* that were linked to penicillin tolerance in *Staphylococcus aureus* [13]. A

previous lab member deleted *lrgAB* in *B. anthracis* Sterne and found that the  $\Delta$ *lrgAB* mutant has increased susceptibility to antibacterial agents like LL-37 (a human host defense peptide), daptomycin, and penicillin [10, 14].

While *lrgA* and *lrgB* impact antibacterial susceptibility, the  $\Delta$ ClpX mutant has a stronger phenotype than the  $\Delta$ *lrgAB* mutant [10]. As such, there is the possibility that other genes regulated by ClpXP influence antibiotic susceptibility in *B. anthracis*. Three other genes identified in the microarray analysis were found to be related to the bacterial cell wall: *sigM*, *glpF*, and *msrA* [10]. *sigM* is an extra-cytoplasmic function (ECF) sigma factor that has been found in *Bacillus subtilis* to increase resistance to  $\beta$ -lactam antibiotics, like penicillin, methicillin, and oxacillin, by suppressing a cyclic-di-AMP phosphodiesterase [15, 16]. *glpF*, involved in glycerol uptake, was found to be highly expressed in *S. aureus* for L-form creation and in antibiotic tolerance [17]. Cell wall deficient L-forms are assumed by bacteria when treated with antibiotics [18]. *msrA* codes for a methionine sulfoxide reductase that was found to be upregulated in the presence of oxacillin [19]. Further experiments demonstrated *msrA*'s induction in other cell-wall active antibiotics like bacitracin and D-cycloserine [20].

Given the effectiveness of cell-wall active antibiotics on *B. anthracis* and the relationships between the three genes and the cell wall, we hypothesize that *msrA*, *sigM*, and *glpF* are playing a role in antibiotic resistance in *B. anthracis*. To test this hypothesis, we will first confirm that these genes are regulated by ClpX and then we will create knock-out mutants to determine their role in antibiotic resistance and virulence.

## METHODS

**Table 1. List of primers used in this study.** Unless otherwise noted, all primers were used at a concentration of 10  $\mu$ M.

<i>SigM</i> QPCR Fwd-2	5'-CTG TGA TAG AGG CAC AAG CTG TT-3'
<i>SigM</i> QPCR Rev-2	5'-ACA GAA GCA CCC TCT TCG TAC-3'
<i>GlpF</i> QPCR Fwd	5'-CAG GAT ACG CAA TCA ACC CAG-3'
<i>GlpF</i> QPCR Rev	5'-CGG ACC TAC TAC TGG AAT CCA TG-3'
<i>MsrA</i> QPCR Fwd	5'-CGA CGG GAC ATT ATG AGG CA-3'
<i>MsrA</i> QPCR Rev	5'-ATT GCC CGC CTA CAT CAG TC-3'
<i>SigM</i> IM Fwd-XhoI	5'-ACA GTC TCG AGC CTT TCT CGT AGC CAT CAT GC-3'
<i>SigM</i> IM Rev-HINDIII	5'-GAC TAA GCT TTG CCT CTA ATT CCT CCG TTC C-3'
<i>GlpF</i> IM Fwd-XhoI	5'-ACA GTC TCG AGA CGT GGT TGG ATC AAT TAG TGG- 3'
<i>GlpF</i> IM Rev-HINDIII	5'-GAC TAA GCT TCC TGT CGT TCC ACC TAA TGA T-3'
pHY304Fwd	5'-ACG ACT CAC TAT AGG GCG AAT TGG-3'
pHY304 Rev	5'-GCG GAT AAC AAT TTC ACA CAG G-3'

### Qualitative Reverse Transcriptase PCR (QPCR)

Wild-type and  $\Delta$ ClpX RNA was transcribed into complementary DNA using 20  $\mu$ l RNA (200 ng/ $\mu$ l) and 20  $\mu$ l of a mixture comprising of 4  $\mu$ l Reverse Transcriptase (RT) buffer, 4  $\mu$ l random primers, 1.6  $\mu$ l 25x ribonucleic triphosphates (rNTP), 4  $\mu$ l of RT enzyme, 2  $\mu$ l of RNase inhibitor, and 4.4  $\mu$ l of water following manufacturer's protocols (Superscript II, Life Technologies). The combined 40  $\mu$ l of PCR product was then diluted 1:10. 5  $\mu$ l of the cDNA dilution was mixed with 15  $\mu$ l of a primer mixture constituting 10  $\mu$ l Sybr Green dye, 0.5  $\mu$ l 10

$\mu$ M Fwd primer, 0.5  $\mu$ l 10  $\mu$ M Rev primer, and 4  $\mu$ l of water. This mixture was run through QPCR utilizing the ddCT relative quantitation assay with dissociation stage. Each individual trial had 3 replicate wells for wild-type and  $\Delta$ ClpX. In total, three biologically independent trials were utilized per gene.

### Primer Efficiency

Complementary genomic DNA was created in a similar fashion for the above RT-QPCR analysis. cDNA was then diluted into 1:5, 1:50, 1:500 dilutions of cDNA. As above, 5  $\mu$ l of the cDNA was mixed with 15  $\mu$ l of the same mix of Sybr Green dye, Forward (Fwd) and Reverse (Rev) primers, and water. Each dilution was replicated 3 times within a trial, and the final mixture was induced in the QPCR machine. Results were then graphed, with the inverse slope inserted into a formula provided by ThermoFisher Scientific (<https://www.thermofisher.com/us/en/home/brands/thermo-scientific/molecular-biology/molecular-biology-learning-center/molecular-biology-resource-library/thermo-scientific-web-tools/qpcr-efficiency-calculator.html>) which gave the primer efficiency for each set of experimental primers.

### Insertional Mutants

Insertional mutants of *sigM* and *glpF* were created using the pHY304 plasmid. Several steps were utilized: Creating the mutagenesis plasmid, transforming into GM2163, transforming into *B. anthracis* Sterne and temperature shifting.

*Creating the mutagenesis plasmid*

The *sigM* and *glpF* insertions were amplified in PCR reactions that included 2.5  $\mu$ l of colony WT DNA (a WT colony with 10  $\mu$ l water, microwaved for 1 minute), 2.5  $\mu$ l of *sigM* or *glpF* Insertional Mutant (IM) Fwd, 2.5  $\mu$ l of *sigM*/*glpF*-IM Rev primers, 5  $\mu$ l of 10x buffer, 5  $\mu$ l of 10x dNTP, 2.5  $\mu$ l of PFU polymerase, and 30  $\mu$ l of water using 54  $^{\circ}$ C annealing temperature followed by 1 min extension at 72  $^{\circ}$ C. Two 50  $\mu$ l reactions were made for each insert and then combined after PCR amplification. The combined 100  $\mu$ l of PCR product had 17  $\mu$ l of loading dye added. Gel electrophoresis was run to confirm PCR amplification. The PCR product was purified using a Wizard Gel and PCR Cleaning Kit (Promega) following manufacturer's instructions for both *sigM* and *glpF*.

The purified PCR products of the *sigM* and *glpF* genes were then digested by mixing the following: 5  $\mu$ l of buffer 2.1 (10x) was added to 1  $\mu$ l of Xho1, 1  $\mu$ l of HindIII, and 43  $\mu$ l of purified PCR product mixture. Since neither PCR product had 43  $\mu$ l of total volume, 40  $\mu$ l of *sigM* PCR product was added with 3  $\mu$ l of water, and 38  $\mu$ l of *glpF* was added to 5  $\mu$ l of water to reach the desired quantity. The pHY304 plasmid mixture included 5  $\mu$ l of buffer 2.1, 2  $\mu$ l of Xho1, 2  $\mu$ l of HINDIII, 8  $\mu$ l of pHY304 (844 ng/ $\mu$ l), and 33  $\mu$ l of water. The two 50  $\mu$ l mixtures were both incubated at 37  $^{\circ}$ C for 3-4 hours, with 1  $\mu$ l of CIP added for 30 minutes at the end of that period for the pHY304 plasmid mixture. Afterwards, the restriction digest products were purified in the same way as aforementioned PCR products.

After digesting the *sigM* and *glpF* insert DNA as well as the pHY304 plasmid, the two were combined in a ligation. For *sigM*, 4  $\mu$ l of pHY304 (12.4 ng/ $\mu$ l) were added with 1  $\mu$ l of *sigM* (12.5 ng/ $\mu$ l), 2  $\mu$ l of 10x ligation buffer, 1  $\mu$ l of T4 ligase, and 12  $\mu$ l of water. For *glpF*, 1  $\mu$ l of *glpF* (17.5 ng/ $\mu$ l) was added to 3  $\mu$ l of pHY304 (12.4 ng/ $\mu$ l), 2  $\mu$ l of 10x ligation buffer, 1  $\mu$ l T4 ligase, and 13  $\mu$ l of water. Two negative controls were also included, using the same

mixtures as above, but without the *sigM* or *glpF* insert DNA. Ligations were incubated at room temperature overnight.

#### *Transformation of GlpF-IM plasmid into GM2163*

The *glpF*-IM ligation was transformed into the MC1061 *E. coli* strain (Lucigen). The electrocompetent bacteria were thawed on ice, and 2  $\mu$ l of ligation was added with 25  $\mu$ l of the bacteria. It was kept in the ice for ten minutes, after which the mixture was transferred to the electroporation cuvette and run through the electroporator on a voltage of 1800 mV. Immediately after, 950  $\mu$ l of recovery media was added. This new mixture was incubated at 30 °C for 1.5 hours. 100  $\mu$ l of the transformation was plated onto BHI plates containing the antibiotic erythromycin at 500  $\mu$ g/ml (Erm500). The presence of the ligated plasmid was confirmed in the resulting colonies by PCR with the pHY Fwd and Rev primers (10  $\mu$ M) and the resulting bands were analyzed by gel electrophoresis. Upon confirmation, the plasmid was purified using the IBI plasmid kit, and then transformed into unmethylated electrocompetent GM2163 cells using the same process as for the MC1061F cells.

#### *Transformation of SigM-IM plasmid into GM2163*

Unlike *glpF*, the *sigM*-IM plasmid was transformed with chemically competent NEB5- $\alpha$  cells. The *E. coli* cells were thawed on ice, and 100  $\mu$ l of ligation was added to a tube of the NEB5-alpha cells, which stayed in the ice for 30 minutes. The mixture was heated at 42 °C for 30 seconds and then placed on ice for 5 minutes. 900  $\mu$ l of SOC media was added to a culture tube and the combined cells, DNA, and media were incubated at 30 °C for 2 hours. The cells were plated on Erm500 plates and screened via PCR. Afterwards, the plasmid was transferred to GM2163 in a similar manner as the *sigM*-IM plasmid.

#### *Transformation into B. anthracis and temperature shifting.*

*B. anthracis* cultures were grown overnight in 3 mL of BHI, shaking at 37 °C. 0.5 mL of the overnight culture was transferred to 50 ml of BHI in a 500 mL flask and incubated at around 200 rpm shaking at 37 °C shaking. The optical density (OD) was then measured using a wavelength of 600 nm. After reaching an OD of 0.6-0.8 bacterial cells were collected in 500 mL sterile filters via vacuum. Cells were washed with 25 mL of ice-cold electroporation buffer, repeated a total of three times. The cells were resuspended in 2.5 mL of buffer and put on ice. Around 500 ng of unmethylated plasmid DNA for both mutants was added to 80 µl of the *B. anthracis* cells in an electroporation cuvette. The mixture was kept in ice for around 15 minutes and then pulsed at 1.8 kV. Immediately, 500 µl of recovery media was added to the mixture and transferred to plastic tubes. They were then incubated at 30 °C for 1.5 hours. The results were then plated on Erm5 plates and grown overnight at 30 °C. Colonies were chosen and plated onto an Erm5 reference plate and screened for presence of the mutagenesis plasmid using the pHY Fwd and Rev primers.

To temperature shift *B. anthracis*, overnight cultures were grown at 30 °C in BHI with erythromycin. The next morning, 100 µl of the overnight cultures were added to 5 mL of Erm5 BHI and grown at 37 °C for 8 hours. These cultures were then diluted into 1:500, 1:1000, and 1:5000 and 100 µl was plated onto Erm5 BHI plates. They were then grown overnight at 37 °C. PCR was run on resulting colonies to confirm creation of the mutant using colony DNA and the pHY304 Fwd and QPCR rev primer for either *sigM* or *glpF*. The final mutants were stored in the -80 °C freezer in a 20% glycerol solution.

#### Minimum Inhibitory Concentration Assay

Overnight cultures were prepared using 3 mL of Brain-Heart Infusion (BHI) media and 10  $\mu$ L of frozen bacterial stocks for wild-type,  $\Delta$ ClpX,  $\Delta$ SigM, and  $\Delta$ GlpF. Cultures were grown and shaken at 37 °C for 16-17 hours. Cultures were diluted into a final concentration of 1:100 in BHI and added to penicillin with a final concentration of either 80, 40, 20, 10, 5, 2.5, 1.25, 0.63, 0.3, 0.15 or 0  $\mu$ g/ml of penicillin in BHI with a final volume of 200  $\mu$ l in a 96-well flat bottom plate. The bacteria were then grown at 37 °C under static conditions for 20 hours and the OD was measured.

Daptomycin MIC assays were prepared in a similar way. Overnight cultures of wild-type,  $\Delta$ ClpX,  $\Delta$ SigM, and  $\Delta$ GlpF were grown in 3 mL of BHI media for 16-17 hours. The bacterial media were pelleted via centrifugation and the supernatant removed and replaced with 3 mL of Mueller Hinton Broth II (MHB) with 50  $\mu$ g/ml of CaCl<sub>2</sub> to make CA-MHB media. Daptomycin final dilutions of 8, 6, 4, 3, 2, and 0  $\mu$ g/ml in CA-MHB were prepared and the bacteria were diluted 1:100 in CA-MHB to a final volume of 200  $\mu$ l in a 96-well round bottom plate. The bacteria were then grown for 20 hours, shaking at 37 °C and the OD was measured.

#### *Galleria mellonella* virulence assay

*G. mellonella* worms were sorted according to weight (190-220 milligrams) into five groups. 12 worms were assigned to wild-type and  $\Delta$ ClpX,  $\Delta$ SigM,  $\Delta$ GlpF, and the PBS control had 10 worms. Overnight cultures of wild-type,  $\Delta$ ClpX,  $\Delta$ SigM, and  $\Delta$ GlpF were grown and log phase cultures were grown to OD 0.4. Next, 1 mL of each bacterial culture was centrifuged at 14,000 rpm and the supernatant replaced with 1 mL of PBS, centrifuged again and the supernatant was removed, and resuspended again in 1 ml of PBS. This was then diluted into a 1:2 solution with more PBS. The starting bacterial counts were checked to ensure no drastic



concentration differences between strains were present. Worms were injected with 10  $\mu$ l of the 1:2 solution. The worms were then stored at 37° C and checked for worm death at 24 hours, 48 hours, and 72 hours.

## RESULTS

We hypothesize that the differences in expression of *sigM*, *glpF*, and *msrA* may explain the changes in antibiotic resistance and virulence of  $\Delta$ ClpX. Our first step was to confirm the microarray results indicating *sigM*, *glpF*, and *msrA* were expressed differently in  $\Delta$ ClpX compared to wild-type *B. anthracis* Sterne via an independent process [10]. We chose qPCR as a way to measure gene expression. Reverse transcriptase converts the RNA in bacterial cells to cDNA and qPCR can precisely measure the amount of DNA present at each cycle during PCR amplification. By quantifying the relative amount of DNA present at a specific time point during logarithmic amplification, we can determine relative starting amounts of cDNA between groups. However, all of this assumes that DNA is doubling every QPCR cycle. If the primers used to create copies of the DNA are not efficient enough to allow doubling with every cycle, then our relative starting amounts may be off. If amplification is doubling every cycle, primer efficiencies ought to be in an effective range of 90-110%.

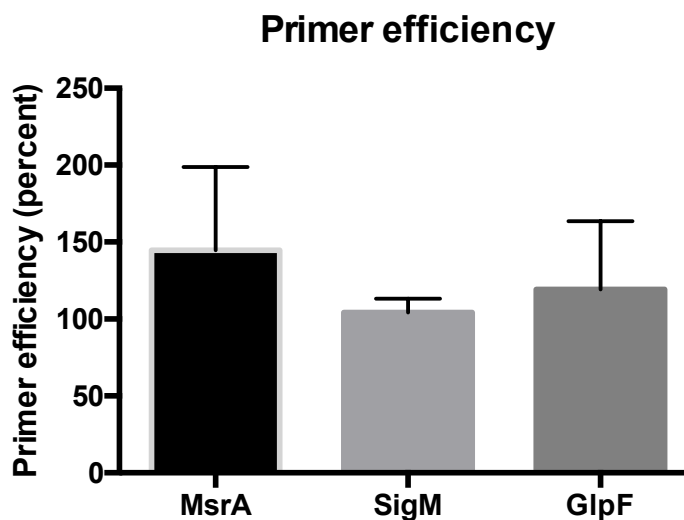


**Figure 1. Primer efficiencies of *MsrA*, *SigM*, and *GlpF* primers.** Data represented with average primer efficiency percent with error bars representing standard deviation. For *msrA* and *glpF*, N=3. For *sigM*, N=2.

Primer efficiencies lower than 100% are indicative of amplification lower than two times the starting amount. Inefficient PCR conditions or primer design could cause this. Primer efficiencies higher than 100% are found with smaller slopes utilized in the formula located in the methods. Amplification is not multiplying by more than two, rather there is some form of polymerase inhibition, contamination, or poor pipetting.

To test primer efficiencies for *sigM*, *glpF*, and *msrA*, we diluted complementary genomic DNA into 1:5, 1:50, and 1:500 dilutions, mixed with primers and Sybr green, and ran QPCR. Only *sigM* fell within the appropriate range, at 104.23% average between the two trials. The others averaged above 110%. Of the two, *glpF* had the more acceptable average, at 119.22%. *MsrA* averaged the highest efficiency at 144.71% (Fig. 1). Despite issues in the primer efficiencies for *glpF* and *msrA*, there were large differences in the relative expression of the three genes in  $\Delta$ ClpX compared to their expressions in WT bacteria (Fig. 2). An expression of 0.1 would mean that the expression in  $\Delta$ ClpX was a tenth that in wild-type. The average for *sigM* was 0.1261, the average for *glpF* was 0.1015, and the average for *msrA* was 5.472 (Fig. 2). We

also included the previously identified gene *lrgA* as a positive control, although only for one trial, which is why there are no error bars (Fig. 2). The data was analyzed via a one sample t-test. All three novel genes demonstrated statistically significant differences in expression between  $\Delta$ ClpX and wild-type. The *p*-value was 0.0012 for *sigM*, 0.0003 for *glpF*, and 0.0392 for *msrA*. This indicated that expression of these genes was significantly altered in  $\Delta$ ClpX and verified the results seen in the original microarray.

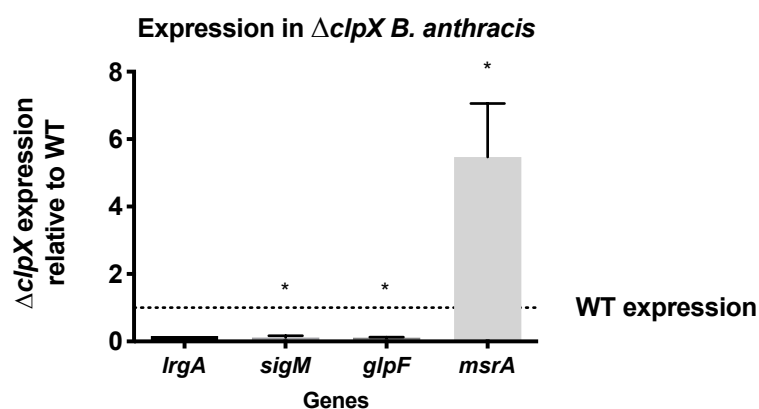


**Figure 2. Expression levels of SigM, GlpF, and MsrA in  $\Delta$ ClpX *B. anthracis* Sterne.** Statistically significant differences demonstrated by \* indicating  $P < 0.05$  via a one-sample T-test. Data represents mean of  $N = 3$  (SigM, GlpF, and MsrA) trials with error bars representing standard deviation. *LrgA* was not included in the statistical analysis because it was only one trial.

Now that we confirmed that these genes were dysregulated in  $\Delta$ ClpX, our next goal was to determine whether any of them are important for antibiotic resistance in *B. anthracis* Sterne. To test this, the genes had to be rendered nonfunctional and the susceptibility of *B. anthracis* Sterne measured without these genes. If the genes were vital to antibiotic resistance in the bacteria, then the nonfunctional mutants would be more susceptible to cell-wall active antibiotics (like penicillin and daptomycin) than wild-type. We chose to focus on the *sigM* gene because sigma factors help initiate transcription via binding to RNA polymerases and therefore can

potentially influence multiple genes [21]. This means that *sigM* could have a wider array of cellular effects than *glpF* or *msrA*. Like *sigM*, *glpF* also had strongly reduced expression in  $\Delta\text{ClpX}$  and so we also decided to construct this insertional mutant concurrently with  $\Delta\text{SigM}$ .

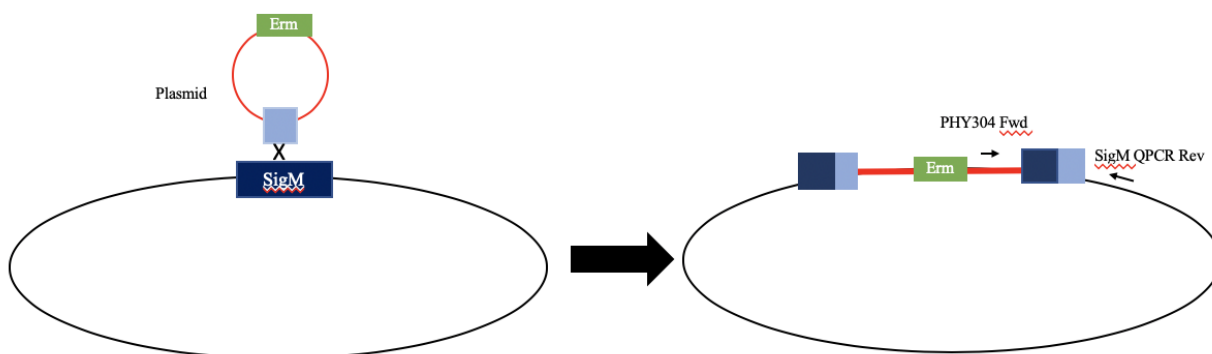


**Figure 3. Schematic of creating the  $\Delta\text{SigM}$  insertional mutant in *B. anthracis* Sterne.** The pPHY304 plasmid (red circle) was inserted into the WT *B. anthracis* Sterne's chromosome (black circle) using homologous recombination. Primers used to confirm integration are shown by the black arrows.

In order to make insertional mutants, two mutagenic plasmids were created by inserting around 400 bps of the middle of the *glpF* gene and around 200 bps of the middle of the *sigM* gene into the temperature sensitive pPHY304 plasmid (left side, Fig 3). These plasmids were transformed consecutively into *E. coli*, unmethylated *E. coli*, and finally *B. anthracis*. When homologous pieces of DNA align, recombination events can occur via homologous recombination. By having a homologous region between the targeted gene and the mutagenic pPHY304 plasmid, the plasmid was able to recombine into the middle of the *sigM* or *glpF* genes effectively disrupting them with a 5000 bp insertion of plasmid DNA (right side, Fig. 3). Homologous recombination was encouraged through the use of temperature shifting that forced plasmid integration and this integration was verified to ensure that the plasmid had indeed entered into the bacterial chromosome and disrupted *sigM*/*glpF*. To verify the insertion and knockout of the *sigM* and *glpF* genes, a PCR using pPHY304 Fwd, a plasmid specific primer, and

a genomic primer downstream of the plasmid insertion site (QPCR Rev for *sigM* and then *glpF*) was performed (small black arrows, Fig. 3). Only if the plasmid was properly inserted into the chromosome could amplification between the pPHY304 Fwd primer and the QPCR reverse primers for both mutants occur. As a control for the specificity of this PCR reaction, we also included wild-type DNA which lacks the inserted plasmid. As can be seen in Fig. 4, wild-type failed to show a band whereas both mutants did. This verified insertion of the plasmid and disruption of the *sigM* and *glpF* genes.

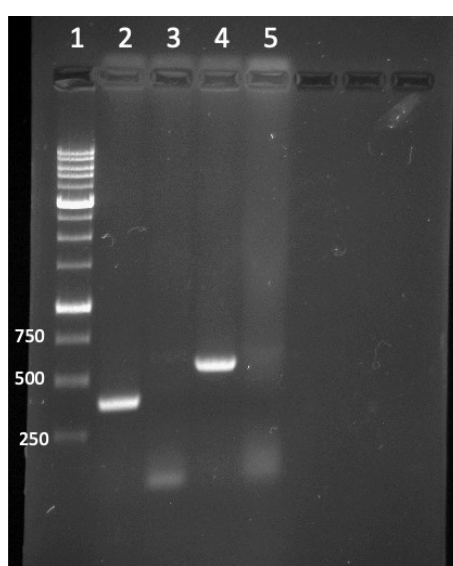


**Figure 4. Gel electrophoresis verifying insertional mutants  $\Delta$ SigM and  $\Delta$ GlpF.** PCR utilizing PHY Fwd and SigM or GlpF QPCR reverse primers. Lanes: (1) Ladder (2)  $\Delta$ SigM DNA + PHY Fwd/SigM Rev. (3) WT DNA + PHY Fwd/SigM Rev. (4)  $\Delta$ GlpF DNA + PHY Fwd/GlpF Rev. (5) WT DNA + PHY Fwd/GlpF Rev. Ladder sizes in base pairs.

In order to test the susceptibility of the new mutants,  $\Delta$ SigM and  $\Delta$ GlpF, to antibiotics MIC assays for cell-wall active antibiotics were performed. The MICs utilized increasing concentrations of a chosen antibiotic to determine at what point the bacteria could no longer grow. This was measured using optical density and would compare the growth of  $\Delta$ SigM and  $\Delta$ GlpF to wild-type and  $\Delta$ ClpX. The more resistant a particular strain of bacteria, the higher the

concentration of antibiotic needed to inhibit them.  $\Delta$ ClpX is known to have decreased susceptibility to penicillin and daptomycin compared to wild-type *B. anthracis* Sterne [9] and serves as a positive control in our assays.

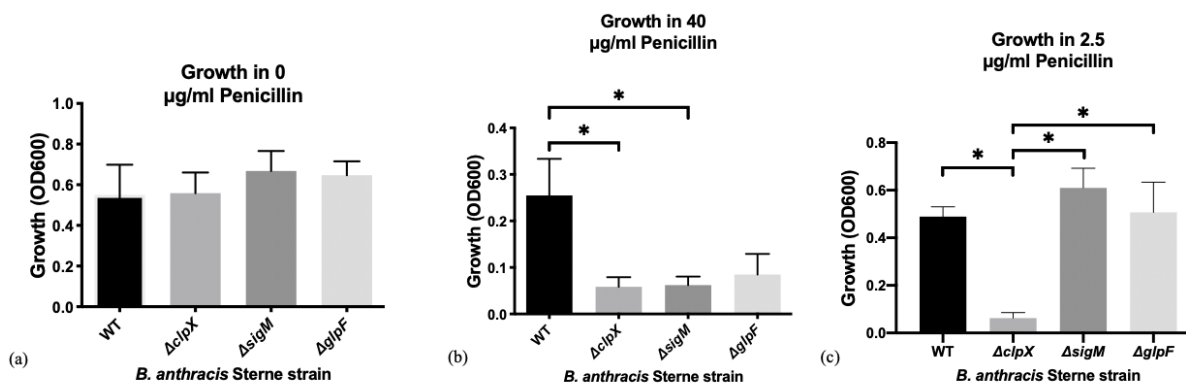


**Figure 5. Loss of *sigM* increases penicillin susceptibility.** Growth of *B. anthracis* Sterne strains WT,  $\Delta$ ClpX,  $\Delta$ SigM, and  $\Delta$ GlpF in an overnight penicillin MIC assay measured at (a) 0 ug/ml penicillin, (b) 40 ug/ml penicillin, and (c) 2.5 ug/ml penicillin. Statistically significant differences demonstrated by \* indicating  $p < 0.05$  via a one-way ANOVA with Tukey-Kramer *post hoc* analysis. Data represents mean of N = 4 trials with error bars representing standard deviation.

For the penicillin MIC assays, the OD for each bacterial strain was analyzed at 0  $\mu$ g/ml, 40  $\mu$ g/ml and 2.5  $\mu$ g/ml penicillin. Comparisons between the strains were made at 0 ug/ml to ensure that differences in OD occurred only when introduced to antibiotics. No statistical significance was observed between any of the bacteria (Fig. 5a), The concentration of 40  $\mu$ g/ml was used because it was the highest concentration where wild-type consistently grew and thus the highest concentration where the mutants could be measured. 2.5  $\mu$ g/ml was used in order to compare the level of susceptibility of  $\Delta$ SigM and  $\Delta$ GlpF to  $\Delta$ ClpX since this was the lowest concentration of penicillin in which  $\Delta$ ClpX was unable to grow. At 40  $\mu$ g/ml, we found that wild-type grew significantly better in the presence of penicillin than either  $\Delta$ ClpX or  $\Delta$ SigM (Fig. 5b). There was no statistically significant difference between wild-type and  $\Delta$ GlpF, with a

$p$ -value at 0.104. At 2.5  $\mu\text{g/ml}$ , we found that  $\Delta\text{ClpX}$  was significantly different from wild-type,  $\Delta\text{SigM}$ , and  $\Delta\text{GlpF}$ . There were no significant differences between wild-type,  $\Delta\text{SigM}$ , or  $\Delta\text{GlpF}$  (Fig. 5c). From these results, we can conclude that the removal of the *sigM* gene increased susceptibility to penicillin, but not as much as the removal of *clpX*

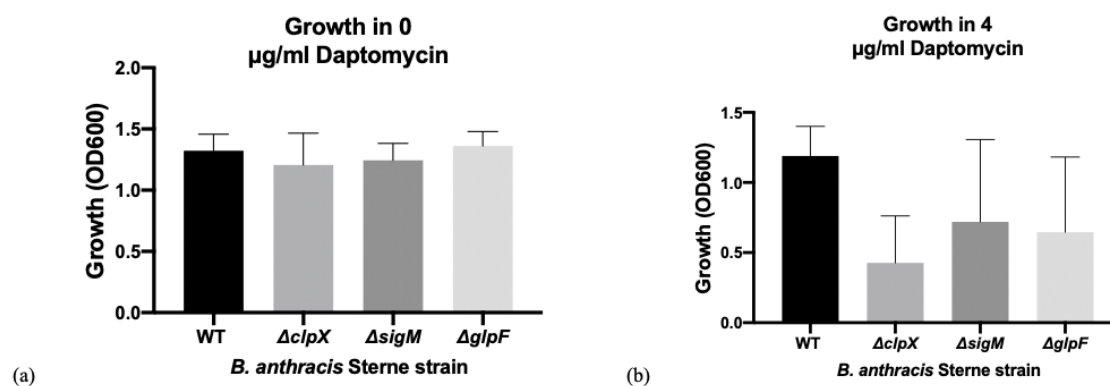


**Figure 6. Loss of *sigM* and *glpF* do not increase daptomycin susceptibility.**

Growth of *B. anthracis* strains WT,  $\Delta\text{ClpX}$ ,  $\Delta\text{SigM}$ , and  $\Delta\text{GlpF}$  in an overnight daptomycin MIC assay measured at (a) 0  $\mu\text{g/ml}$  daptomycin and (b) 4  $\mu\text{g/ml}$  daptomycin. Statistically significant differences demonstrated by \* indicating  $p < 0.05$  via a one-way ANOVA with Tukey-Kramer *post hoc* analysis. Data represents mean of  $N = 3$  trials with error bars representing standard deviation.

For daptomycin MIC assays, OD was measured at 0 and 4  $\mu\text{g/ml}$ . As expected, there was no difference in growth in 0  $\mu\text{g/ml}$  daptomycin (Fig. 6a). However, there was also no statistical significance between any of the four groupings using 4  $\mu\text{g/ml}$  (Fig. 6b). The closest to statistical significance was wild-type compared to  $\Delta\text{ClpX}$  with a  $p$ -value of 0.0665, which based on previous studies [9, 10], and should have been significantly inhibited.  $\Delta\text{SigM}$  compared to wild-type had a  $p$ -value of 0.3776 and  $\Delta\text{GlpF}$  compared to wild-type had a  $p$ -value of 0.3084.

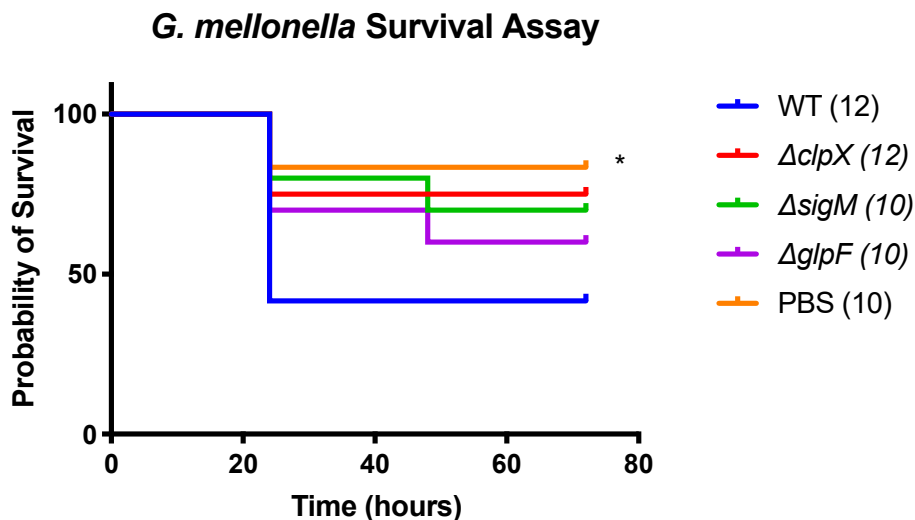


**Figure 7. Survival assay of *G. mellonella*.** Worms were injected with either PBS, WT *B. anthracis* Sterne,  $\Delta ClpX$ ,  $\Delta SigM$ , or  $\Delta GlpF$ . Survival was plotted over 72 hours at 24-hour periods. 10 worms were utilized for  $\Delta SigM$ ,  $\Delta GlpF$ , and PBS and 12 for WT and  $\Delta ClpX$ . Statistically significant differences from wild-type demonstrated by \* indicating  $P < 0.05$  via Log-rank test, Log-rank test for trend, and Gehan-Breslow Wilcoxon test. Data represents values from one trial.

Having analyzed antibiotic susceptibility of the two mutants, it was important to determine if this affected their virulence *in vivo*. Given that  $\Delta ClpX$  is essentially avirulent in several animal models [4, 22], we wanted to see what role either *sigM* or *glpF* played in virulence as loss of these genes could affect more than just antibiotic resistance. The larvae of the greater wax moth, *G. mellonella*, is a well-documented invertebrate infection model that we recently validated for *B. anthracis* Sterne [22]. Using the *G. mellonella* virulence model, the virulence of wild-type,  $\Delta ClpX$ ,  $\Delta SigM$ ,  $\Delta GlpF$ , and PBS was tested. After 72 hours, 42% of WT-injected worms survived, 75% of the  $\Delta ClpX$ -injected worms survived and 83.3% of the PBS worms survived. This consistent with our previously published results for these groups [22]. We also found that 70% of the  $\Delta SigM$ -injected worms survived and 60% of the  $\Delta GlpF$ -injected worms survived (Fig. 7). However, despite these high survival rates, there was no statistical



significance between survival of the wild-type group and any of the 3 mutant strains ( $\Delta$ ClpX,  $\Delta$ SigM, or  $\Delta$ GlpF). The only statistically significant difference in survival is seen in the PBS-injected control group. Therefore, we cannot definitively conclude that any of these mutants have a virulence phenotype without increasing our sample size by repeating these experiments.

## DISCUSSION

Previous studies have demonstrated that loss of *clpX* results in loss of antibiotic resistance to cell-wall active antibiotics [8,9]. The goal of this study to investigate genes downstream of ClpX that might be mediating this effect. I focused on *msrA*, *glpF*, and *sigM* because gene expression was vastly altered in the  $\Delta$ ClpX mutant in a recent microarray study [9]. Our initial hypothesis was that *sigM*, *glpF*, and *msrA* played a role in the antibiotic resistance of *B. anthracis* Sterne as well as virulence based their different expressions in  $\Delta$ ClpX compared to wild-type and their previously described links to antibiotic resistance. We began our study by confirming *sigM* and *glpF* are downregulated in  $\Delta$ ClpX compared to wild-type while *msrA* is upregulated. One caveat in our results is that only *sigM*'s primers were within the normal efficiency range of 90-110%. The other two genes had primer efficiencies greater than 110%. While not ideal, it is unlikely to change our conclusions as the difference in gene expression of *glpF* and *msrA* were so great. However, retesting these primer efficiencies would be beneficial to confirm that inefficient primer amplification is not inadvertently skewing our results.

Knockout mutants for *glpF* and *sigM* were made using insertional mutagenesis. The phenotypes of these mutants were assessed using MIC assays for penicillin and daptomycin to determine whether the absence of *sigM* or *glpF* resulted in increased antibiotic susceptibility. For penicillin,  $\Delta$ SigM showed statistically significant loss of growth at 40  $\mu$ g/ml compared to wild-

type and significantly more growth than  $\Delta\text{ClpX}$  at 2.5  $\mu\text{g/ml}$ . This indicated that while  $\Delta\text{SigM}$  was more susceptible to antibiotics than wild-type, it was not more susceptible than  $\Delta\text{ClpX}$  since growth of  $\Delta\text{SigM}$  is unaffected by 2.5  $\mu\text{g/ml}$  but growth of  $\Delta\text{ClpX}$  is completely inhibited. For  $\Delta\text{GlpF}$ , there was no statistically significant difference in growth from wild-type. However, only in one out of our four experiments did  $\Delta\text{GlpF}$  actually grow at 40  $\mu\text{g/ml}$ . In the other three experiments, it did not grow. Therefore, it is possible that with further optimization of our assays, we may see a more consistent phenotype in growth of  $\Delta\text{GlpF}$  in penicillin.

Our daptomycin MIC assays were problematic. Variations between assays were high, as can be seen in the large error bars in Fig. 6b. Wild-type *B. anthracis* Sterne was not significantly different from any of the mutants at 4  $\mu\text{g/ml}$ . This is problematic because it has already been shown that  $\Delta\text{ClpX}$  has increased susceptibility to daptomycin [9, 10]. This was not the case in our daptomycin MIC assays. Given the problems with acquiring consistent results and an inability to see differences between wild-type and  $\Delta\text{ClpX}$ , which essentially serves as a positive control for the assay, no real conclusions could be drawn about antibiotic susceptibility for the mutants in daptomycin. It is uncertain why the daptomycin assay yielded unclear results. Perhaps it had to do with the cultures being overnight where bacteria had reached stationary phase and were likely no longer metabolically active. Previous studies in lab had used younger bacterial cultures still in the logarithmic phase of growth for MIC assays [9, 10]. It is possible that this disturbed the effectiveness of daptomycin to some extent. It is also possible that the daptomycin samples used were somehow compromised or there were issues with media preparation. As such, given the failure to achieve technical proficiency with this assay, further testing would be needed to better determine whether *sigM* or *glpF* plays a role in daptomycin resistance.

In order to compare the impact on virulence of *sigM* and *glpF*, survival assays were run on the *G. mellonella* invertebrate worm model. Unfortunately, only one trial of the survival assay was completed with another trial canceled due to the COVID-19 pandemic. While no statistical difference was determined between the  $\Delta$ SigM and  $\Delta$ GlpF, there was a noticeable difference in survivability of the worm models comparable to wild-type. Additionally  $\Delta$ ClpX is not significantly different from wild-type in these results either even though  $\Delta$ ClpX is well-documented to have virulence phenotypes in both the *G. mellonella* [21] as well as mammalian infection models [4, 22]. As such, it is not unreasonable to speculate that with further trials, *sigM*, *glpF*, or both could have been found to have statistically significant difference from wild-type.

There are several additional follow-up studies planned for  $\Delta$ SigM. These include genetic complementation to definitively show that loss of *sigM* is responsible for the observed phenotypes, expanding the classes and types of antibiotics we will test on  $\Delta$ SigM and repeating our *G. mellonella* virulence assays. If *sigM* continues to demonstrate an effect on antibiotic resistance, then efforts should be made to determine the mechanism behind that action. Like ClpX, SigM affects multiple genes. In previous studies, SigM was found to affect several genes in *Bacillus subtilis* related to cell wall synthesis as well as other genes like *gdpP* phosphodiesterase and *disA*, a deadenylate cyclase [16]. It would be useful to determine if these genes and others are also affected in *B. anthracis* and to what extent these genes affect the antibiotic resistance of *B. anthracis* Sterne.

Overall, our results indicate that *sigM* plays a role in antibiotic resistance in *B. anthracis* Sterne. Loss of *clpX* would result in lower expression levels of *sigM* and this may account, in part, for the increased susceptibility to antibiotics seen in  $\Delta$ ClpX. However, *sigM* does not single

handedly contribute to this. Given that  $\Delta\text{ClpX}$  reached its minimum inhibitory concentration before  $\Delta\text{SigM}$  did, this indicates that *sigM* influences antibiotic resistance to a lesser degree than  $\Delta\text{ClpX}$  and is one of likely several genes, such as *lrgAB*, that are found within the ClpX regulatory network that contribute to antibiotic resistance [10]. Further research will explore on other genes, such as *msrA*, that may also contribute to antibiotic resistance. This research will provide better information on how ClpX mediates antibiotic resistance. The ClpXP protease has been proposed as an antibiotic target because of the necessity of this protease for regulating protein turnover [23]. It will be important to better understand the regulatory network of this protease and how it could be exploited for potential drug targets even against more resistant species of bacteria.

REFERENCES

1. Dixon, T.C., et al., *Anthrax*. N Engl J Med, 1999. **341**(11): p. 815-26.
2. Manchee, R.J., et al., *Formaldehyde Solution Effectively Inactivates Spores of *Bacillus anthracis* on the Scottish Island of Gruinard*. Applied and Environmental Microbiology, 1994. **60**(11): p. 4167-4171.
3. Bryskier, A., *Bacillus anthracis and antibacterial agents*. Clinical Microbiology and Infection, 2002. **8**(8): p. 467-478.
4. McGillivray, S.M., et al., *ClpX Contributes to Innate Defense Peptide Resistance and Virulence Phenotypes of Bacillus anthracis*. Journal of Innate Immunity, 2009. **1**(5): p. 494-506.
5. Frees, D., et al., *Clp ATPases and ClpP proteolytic complexes regulate vital biological processes in low GC, Gram-positive bacteria*. Molecular Microbiology, 2007. **63**(5): p. 1285-1295.
6. Baker, T.A. and R.T. Sauer, *ClpXP, an ATP-powered unfolding and protein-degradation machine*. Biochimica et Biophysica Acta (BBA) - Molecular Cell Research, 2012. **1823**(1): p. 15-28.
7. Truscott, K.N., A. Bezawork-Geleta, and D.A. Dougan, *Unfolded Protein Responses in Bacteria and Mitochondria: A Central Role for the ClpXP Machine*. Iubmb Life, 2011. **63**(11): p. 955-963.
8. Kajfasz, J.K., J. Abranches, and J.A. Lemos, *Transcriptome analysis reveals that ClpXP proteolysis controls key virulence properties of Streptococcus mutans*. Microbiology, 2011. **157**(10): p. 2880-2890.

9. McGillivray, S.M., et al., *Pharmacological Inhibition of the ClpXP Protease Increases Bacterial Susceptibility to Host Cathelicidin Antimicrobial Peptides and Cell Envelope-Active Antibiotics*. *Antimicrobial Agents and Chemotherapy*, 2012. **56**(4): p. 1854-1861.
10. Claunch, K.M., et al., *Transcriptional profiling of the clpX mutant in Bacillus anthracis reveals regulatory connection with the lrgAB operon*. *Microbiology-Sgm*, 2018. **164**(4): p. 659-669.
11. Nikolaidis, I., S. Favini-Stabile, and A. Dessen, *Resistance to antibiotics targeted to the bacterial cell wall*. *Protein Science*, 2014. **23**(3): p. 243-259.
12. Bayer, A.S., T. Schneider, and H.G. Sahl, *Mechanisms of daptomycin resistance in Staphylococcus aureus: role of the cell membrane and cell wall*, in *Antimicrobial Therapeutics Reviews: The Bacterial Cell Wall as an Antimicrobial Target*, K. Bush, Editor. 2013, Blackwell Science Publ: Oxford. p. 139-158.
13. Groicher, K.H., et al., *The Staphylococcus aureus lrgAB operon modulates murein hydrolase activity and penicillin tolerance*. *Journal of Bacteriology*, 2000. **182**(7): p. 1794-1801.
14. Hancock, R.E.W. and H.G. Sahl, *Antimicrobial and host-defense peptides as new anti infective therapeutic strategies*. *Nature Biotechnology*, 2006. **24**(12): p. 1551-1557.
15. Lyon, B.R. and R. Skurray, *Antimicrobial resistance of Staphylococcus aureus: genetic basis*. *Microbiological Reviews*, 1987. **51**(1): p. 88-134.

16. Luo, Y. and J.D. Helmann, *Analysis of the role of Bacillus subtilis sM in ss-lactam resistance reveals an essential role for c-di-AMP in peptidoglycan homeostasis*. *Molecular Microbiology*, 2012. **83**(3): p. 623-639.
17. Han, J., et al., *Glycerol uptake is important for L-form formation and persistence in Staphylococcus aureus*. *PloS one*, 2014. **9**(9): p. e108325-e108325.
18. Strahl, H. and J. Errington, *Bacterial Membranes: Structure, Domains, and Function*, in *Annual Review of Microbiology, Vol 71*, S. Gottesman, Editor. 2017, Annual Reviews: Palo Alto. p. 519-538.
19. Singh, V.K., et al., *Molecular characterization of a chromosomal locus in Staphylococcus aureus that contributes to oxidative defence and is highly induced by the cell-wall-active antibiotic oxacillin*. *Microbiology-Sgm*, 2001. **147**: p. 3037-3045.
20. Utaida, S., et al., *Genome-wide transcriptional profiling of the response of Staphylococcus aureus to cell-wall-active antibiotics reveals a cell-wall-stress stimulon*. *Microbiology-Sgm*, 2003. **149**: p. 2719-2732.
21. Helmann, J.D. and M.J. Chamberlin, *STRUCTURE AND FUNCTION OF BACTERIAL SIGMA FACTORS*. *Annual Review of Biochemistry*, 1988. **57**: p. 839-872.
22. Malmquist, J.A., M.R. Rogan, and S.M. McGillivray, *Galleria mellonella as an Infection Model for Bacillus anthracis Sterne*. *Frontiers in Cellular and Infection Microbiology*, 2019. **9**: p. 9.
23. Brotz-Oesterhelt, H. and P. Sass, *Bacterial caseinolytic proteases as novel targets for antibacterial treatment*. *International Journal of Medical Microbiology*, 2014. **304**(1): p. 23-30.